Primljen / Received: 21.8.2024.
Ispravljen / Corrected: 12.4.2025.
Prihvaćen / Accepted: 26.4.2025.
Dostupno online / Available online: 10.7.2025.

# On the effect of different Eurocode 2-based modelling choices on the calculated fire resistance of RC columns

Authors:

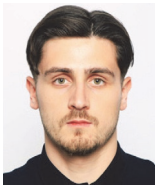

**Marko Rogulj**, MCE
marko.rogulj1998@gmail.com
**Corresponding author**

Prof. **Alen Harapin**, PhD. CE
University of Split
Faculty of Civil Engineering, Architecture and Geodesy
alen.harapin@gradst.hr

Assist.Prof. **Peter Češarek**, PhD. CE
University of Ljubljana, Slovenia
Faculty of Geodesy and Geodesy
peter.cesarek@fgg.uni-lj.si

Assist.Prof. **Jerneja Češarek Kolšek**, PhD. CE
University of Ljubljana, Slovenia
Faculty of Geodesy and Geodesy
jerneja.cesarek-kolsek@fgg.uni-lj.si

Research Paper

Marko Rogulj, Alen Harapin, Peter Češarek, Jerneja Češarek Kolšek

## On the effect of different Eurocode 2-based modelling choices on the calculated fire resistance of RC columns

This paper examines the impact of different modelling choices on the fire performance of RC columns using Eurocode 2 in a real-world case study. The methodology includes a comparative analysis of simplified and advanced numerical simulations, employing FDS for fire curves and ABAQUS for thermal and mechanical analyses. Results show how modelling assumptions affect load-bearing capacity and fire resistance. Conclusions emphasise balancing safety and efficiency, highlighting the importance of variable axial loads and multiple heat zones for accurate fire resistance assessment.

**Key words:**
**fire analysis, RC column, simplified procedures, advanced procedures, natural fires, EC2**

Prethodno priopćenje

Marko Rogulj, Alen Harapin, Peter Češarek, Jerneja Češarek Kolšek

## Utjecaj različitih modelskih pristupa temeljenih na Eurokodu 2 na proračunanu požarnu otpornost AB stupova

Ovaj rad istražuje utjecaj različitih modelskih pristupa na otpornost armiranobetonskih stupova na požar prema Eurokodu 2, primjenjujući ih na stvarnome primjeru iz prakse. Metodologija uključuje usporednu analizu pojednostavljenih i naprednih numeričkih simulacija, pri čemu se računalni program FDS (engl. Fire Dynamics Simulator) koristi za određivanje požarnih krivulja, a računalni program ABAQUS za toplinske i mehaničke analize. Rezultati pokazuju kako pretpostavke u modeliranju utječu na nosivost i otpornost na požar. Zaključci ističu potrebu za ravnotežom između sigurnosti i učinkovitosti te važnost varijabilnih osnih opterećenja i više toplinskih zona za točnu procjenu otpornosti na požar.

**Ključne riječi:**
**požarna analiza, armiranobetonski stup, pojednostavljene metode, napredne metode, prirodni požari, EC2**

## 1. Introduction

In accordance with the requirements of EN 1992-1-2:2004 [1], fire analyses of reinforced concrete (RC) columns can be carried out in various ways with different degrees of precision. Among the latter, the so-called member-analysis methods still seem to prevail in practice. As already implied by their name, these are the methods where the RC column is only considered as a single (isolated) structural element, and the influence of the surrounding structure on it is only described via the forces and moments applied at the ends of the element and via specifically defined kinematic boundary conditions. On top of this, the following simplifications are also often included:

- The boundary forces on the column are considered to remain constant during a fire, and so are the boundary conditions.
- The change in temperatures of the surroundings of the column is defined by a so-called nominal fire curve from EN 1991-1-2:2002 [2]. The latter depends on time and on the general type of the expected fire (standard, external, or hydrocarbon fire), but it does not also depend on the specifics of the analysed fire compartment (e.g., its floor area, volume, quantity and distribution of openings, and flammable obstructions, etc.), although these are also known to influence the fire dynamics. Furthermore, among the nominal fire curves, the so-called standard fire curve is applied in most cases.
- It is assumed that the temperature of the surroundings of the column at a given time of the fire is constant along the height of the column and around its perimeter.
- The convection and radiation heat fluxes that are generated during the fire at the contact between the column and its surroundings are calculated based on the recommendations on convection and radiation coefficients according to EN 1991-1-2:2002 [2] and EN 1992-1-2:2004 [1], respectively.
- Deformations of the column are described by the equations of a 2nd-order solid mechanics theory method instead of the equations of a more reliable geometrically nonlinear theory procedure. In addition, rough compensation is often made for the effects of high temperatures by accounting for a reduced size of the concrete cross-section instead of the actual one. The reduced concrete part of the column's cross-section is considered to remain at its initial (ambient) temperature at all times of the fire and is normally defined by the so-called 500 °C isotherm method or the zone method as proposed by EN 1992-1-2:2004 [1].

By now, many engineers have become aware that, in some cases, the assumptions listed above may underestimate the fire resistance of the column. While these assumptions are "safe," they can lead to unnecessarily expensive engineering solutions (e.g. to a specification of highly excessive structural fire protection), and these could be avoided to some extent by omitting at least some of the simplifications. In contrast, some of the assumptions may overestimate the fire resistance of the columns and may be "unsafe". Unfortunately, it seems that up until today it has not yet been sufficiently clarified which of these simplifications should be eliminated first (i.e. which have the greatest influence on the conservatism of the computed result or are, in contrast, potentially unsafe). This question will be addressed in this paper. To add additional credibility to the study, the investigation will be performed on a case of a selected (real) RC building and a real fire that broke out in this building in late 2016 and was described in [3, 4].

## 2. Material and methods

### 2.1. Preliminary work

The study of this paper is a continuation of a part of the results gathered in the scope of the postdoctoral project [3]. The study also represents a fine-tuning and an upgrade of the preliminary work done in the scope of the master's thesis of Rogulj [5]. The analyses presented in [5] were done primarily on numerical models applying relatively coarse finite element meshes. These were adapted to the available computer equipment of the student, software licensing limitations, and the time frames available for completion of the thesis. Other adaptations of the models, such as neglecting the contribution of the steel reinforcement to the load-bearing capacity of the compressed concrete of the column, were also applied for the same reason. To further enhance the reliability of our conclusions, however, the mentioned adaptations were omitted in the analyses reported in this paper, and the study was repeated and further extended.

### 2.2. Case study

An RC building owned by a company for sales and repair of cars is analysed, where a fire breaks out in a part of its basement. It is assumed that this part of the basement is the same as the part of the basement of the RC building in Jesenice (Slovenia) where a massive fire occurred at the end of 2016, as reported in [3, 4]. Based on the data available in these sources, the same characteristics are adopted for the allegedly affected fire compartment of the building discussed in this paper, i.e. its load-bearing structure, its geometric characteristics, distribution of the flammable obstructions, and the arrangement and size of the windows and doors (see Figure 1). However, in contrast to the characteristics of the fire compartment of the real Jesenice building, one fundamental difference is applied, namely, considering the cross-sections of the basement columns. This adjustment is made to align the properties of the columns directly with the goals of this paper and to better serve in the later presentation of our findings. The latter will be further argued in the following sections.

The fire in the building in Jesenice, [3, 4] broke out in a part of its basement with a floor area of around 600 m$^2$ (Figure 1). Around 3000 car tires were stored there at the time of the fire (see the green-marked areas of Figure 1), stacked in piles 2.2 m high, which represented the main fire load.

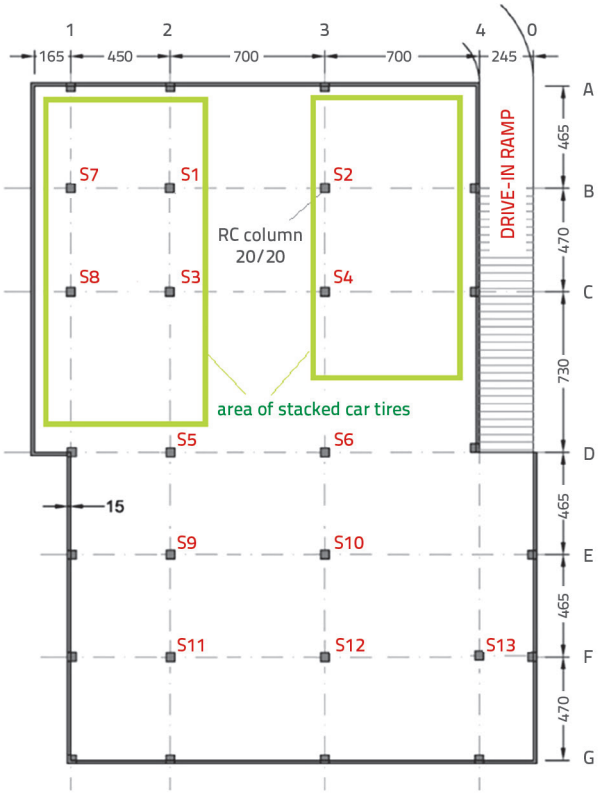


**Figure 1. Floor plan of the fire-affected part of the basement of the analyzed building**

The load-bearing structure of the part of the building shown in Figure 1 is a mixed structural system of RC frames, RC walls and RC slabs. Considering the general purpose of the paper, the fire response of the RC columns of this structure will be discussed. For the sake of brevity, only one column, considered to be one of the most affected columns in the assumed fire, namely column S2, will be analyzed in detail (see Figure 1 for the location of this column).

In the specific case of the building in Jesenice, the RC columns are 3 meters high. This height is adopted also in this paper. However, the cross-section of the real columns is round and has a diameter of 50 cm. As reported in [3, 4], at the start of the 2016 fire, these columns were loaded to only a small fraction (i.e. 10 %) of their cold load-bearing capacity. With such a low load, they were able to withstand the fire easily, as confirmed on-site by the after-fire field inspection of the columns, also reported in [3, 4]. Nevertheless, to increase the probability of the columns not surviving the fire (i.e. collapsing) in the computational fire analyses and thereby allowing a more tangible (i.e. a time-to-collapse-like) comparison between the results of the intended parametric study, columns of a higher slenderness will be considered with steel reinforcement as presented in Figure 2. Concrete is defined as grade C30/37 and reinforcing steel is specified as grade B 500. Although columns with a 20 cm × 20 cm cross-section, as selected in this paper, seem less common in real buildings, they still possess possible geometrical features of columns in buildings where the following two conditions are met simultaneously:

- The horizontal actions of wind and (if relevant) earthquake are taken over primarily by RC walls of the building. The RC columns are of secondary importance and do not contribute to overtaking the horizontal loading.
- Other (local) horizontal actions, such as impacts of vehicles, are not relevant for the building.

While the first condition would be met, for example, if a sufficient portion of massive RC walls were included in the overall building load-bearing system, the second condition would require that no movement of vehicles is possible inside the building. Although the latter condition is not met for the real Jesenice building, it is assumed to be met for the building discussed in this paper. In this respect, the building discussed cannot be considered as a building intended for the sale and service of cars per se, but rather as an auxiliary building for a company engaged in such activities (e.g. a building offering office spaces for the company and with a basement for multi-purpose storage).

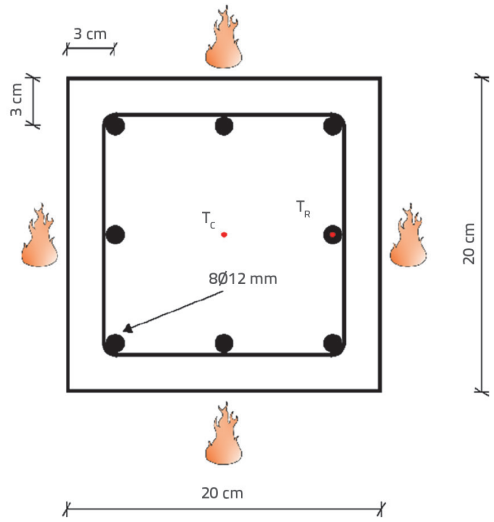


**Figure 2. Assumed cross-section of the analyzed RC column**

Furthermore, a concentric load $N_{0,Ed}$ = 1000 kN is assumed to act on the top of the observed column S2. Depending on the specifics of the rest of the structural system of the building, this load can be considered to represent a portion of the design axial force of the column corresponding to the Eurocode's fundamental combination of actions [6].

A concentric load $N_{0,Ed}$ = 1000 kN was calculated for the observed column S2, based on assumptions representing the real building:

- the building is of a type B+U+2F (basement + ground floor + 2 upper floors),
- the geometric and load-bearing features of the relevant parts of all floors (including the roof) above column S2 are all identical and equal to the ones shown in Figure 1, the relevant areas of the floor slab that affect the axial load of column S2 can be considered as roughly representing a half of the areas lying between axes 2 and 4 and axes A and C in this figure.

- The relevant actions accounted for the building in accordance with EN 1991-1-1 [7] were taken as $g_k$ = 5,8 kN/m² (permanent actions), $q_{k,1}$= 2.5 kN/m² (imposed actions), and $q_{k,2}$ = 1,21 kN/m² (snow action representing a typical value relevant for lower elevation regions of central Slovenia with the corresponding combination factor $\psi_{1,2}$ = 0.5).

This load can be considered to represent a portion of the design axial force of the column corresponding to the Eurocode's fundamental combination of actions [6]. To ensure sufficient load-bearing capacity of the column, the reinforcement of 8 ϕ12 bars was selected. The reinforcement of 8 ϕ12 bars represents 2.3% of the concrete cross-section area, which is marginally above the average between the minimum and maximum values defined by EN 1992-1-1:2004 [20]. This, combined with the assumed dimensions of the column's cross-section and the properties of the concrete, results in the calculated load of the column representing approximately 70% (This value was assessed using a non-linear mechanical model of the column that was composed in Abaqus and was prepared similarly as the model for calculation of the fire response of the column described in Section 2.3.3. The difference was that the analysis was done for ambient temperature conditions, that the loading on the column was not accounted for as to remain constant but as to increase slowly until the detected failure (buckling) of the column and that material properties for concrete and steel reinforcement were reduced as suitable for persistent design situations.) of its ultimate load-bearing capacity, as relevant for persistent design situations according to [6]. Note that such magnitude (i.e. 70%) is in line with the provisions of EN 1992-1-2 [2], which provides instructions for the calculation of the load relevant for fire design of the structure (see Clause 2.4.2.(3) of this standard, Note 2). It is also in line with typical magnitudes of the load applied on columns in standard structural fire testing (EN 1363-1 [8], EN 1365-4 [9]).

## 2.3. Fire analysis of column S2

The fire analysis of column S2 will be divided into the following three essential steps:

Step 1: determination of the temperature of the column's surrounding (fire scenario).
Step 2: determination of concrete temperatures (thermal analysis of the column).
Step 3: determination of the fire resistance of the column (mechanical analysis of the column up until its failure, i.e. collapse).

### 2.3.1. Fire scenario (step 1)

A fire scenario in its most general form means a time- and space-dependent function of temperatures of the surroundings of the fire-exposed structure, i.e. the temperature of the surrounding gas being important for convective transfer of heat to and from the analysed structure and the temperature of the surrounding walls and other obstructions exchanging heat with the structure through radiation. During a fully developed fire, which usually interests us the most from the point of view of the load-bearing capacity of the building's structure, this function can often be simplified to a time-dependent-only function, i.e. a so-called fire curve. With the application of a fire curve along a specific structure (or along a part of it) we accept the assumption that at a certain time *t*, the temperature of the surroundings of the structure will be the same along and around the entire structure.

Considering the fire curves suggested in EN 1991-1-2:2002 [2], a fire engineer may choose between the so-called *nominal fire curves*, which normally only describe the heating but not also the cooling fire phase, or *parametric fire curves* (also: *natural fire curves*). The former are defined by simple analytical expressions, and the latter are most often determined with the help of advanced numerical procedures, for example, in computer programs such as FDS (*Fire Dynamics Simulator*) [10] and others. An analytical expression for the determination of a parametric fire curve is also available in one of the informative annexes of EN 1991-1-2:2002 [2] but this has several limitations and is, thus, only applicable for specific cases of building fires.

When a nominal fire curve of EN 1991-1-2:2002 [2] is applied, this is chosen exclusively based on the general type of the fire, i.e. the *standard fire curve* for a cellulosic fire, the *external fire curve* for a fire affecting an external member of a structure (e.g. a canopy), or the *hydrocarbon fire curve* for a hydrocarbon fire (e.g. a fire in an industrial building). With parametric fire curves, however, other building specifics are also considered, e.g. the size of the fire compartment, the amount and distribution of combustible obstructions, the size and distribution of openings in the building's envelope such as windows and doors (these provide access to fresh air during the fire and may increase the burning rate) etc.

Among the above-mentioned EN 1991-1-2:2002-based [2] nominal fire curves, the *standard fire curve* is used most often in practice because this is also the curve that should be applied in each case according to this standard when not specified otherwise in the requirements of the fire safety designer (to date, unfortunately, the latter still seems to be a frequent scenario in practical engineering). Thus, whenever a nominal fire curve is considered in an analysis in this paper, the standard fire curve will also be applied. However, when a natural fire curve is proposed, this will be generated by fire simulations created with the widely known software FDS. Our FDS simulations will be performed in the software's version 5.5.3 [10] (the reasons for choosing this version are given in what follows) and will combine: (i) analyses of the progressive ignition and burning of combustible obstructions placed around the fire compartment and the corresponding release of heat and gaseous species and (ii) analyses of the transport of heat and gas through the fire compartment and toward the outside (Figure 3). The basis for the simulations of heat and gas transport will be the equations of *computational fluid dynamics* (CFD) *and thermal radiation models*. These are the same equations that are also widely used in other scientific disciplines, such as mechanical engineering and physics; thus, they have received a lot of scientific attention in the past and are now also available for immediate use in many fire engineering software, including FDS. In contrast, however, the models for the

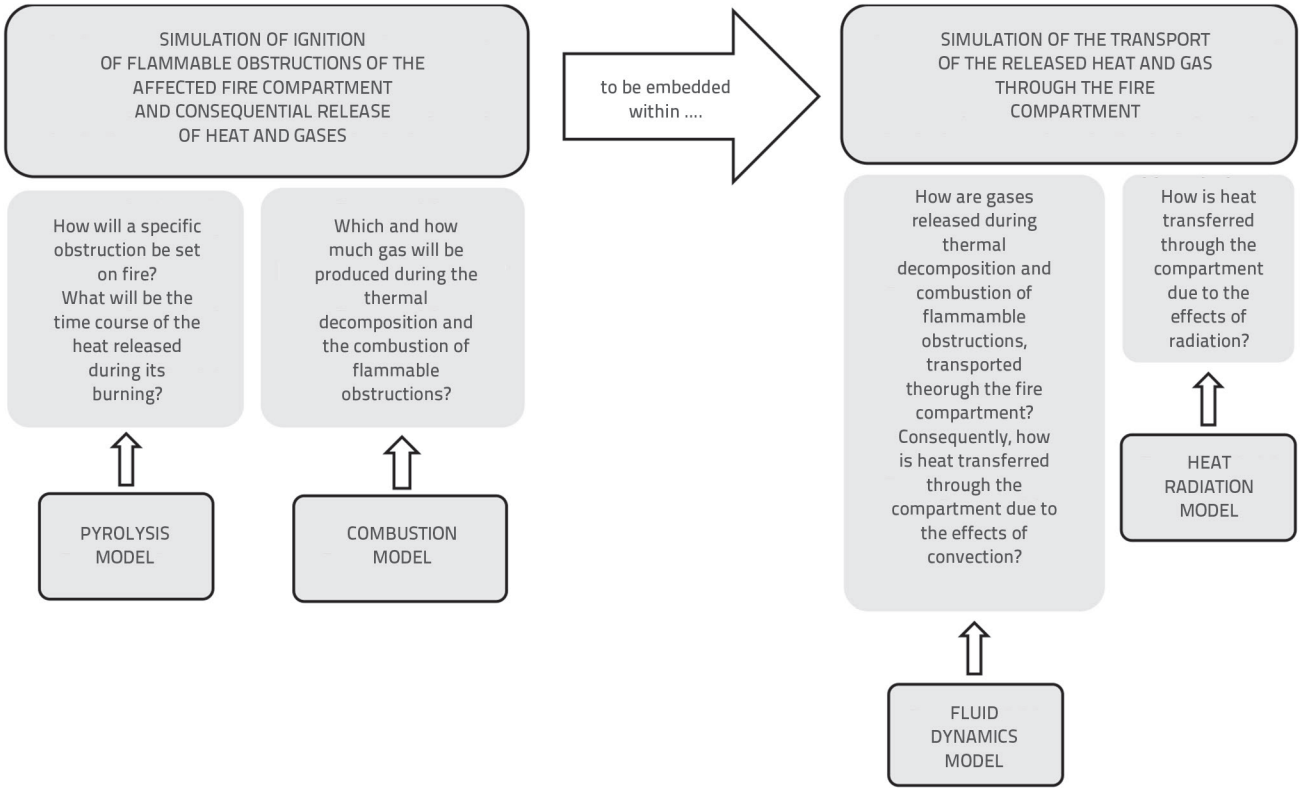


**Figure 3. A general scheme of the computer simulations as used in FDS analyses of this paper for definition of natural fire curves**

ignition of combustible obstructions and the corresponding release of heat (*pyrolysis models*) and gases (*combustion models*) are still under intensive development and are to date in largely the responsibility of each fire safety designer.

**Pyrolysis model**

The pyrolysis rate of a solid material is temperature-dependent and is in FDS [10] governed by two fundamental equations. Firstly, this is the Arrhenius equation which considers each material to be distinguished by several types of intermolecular bonds which are breaking down at different temperatures. The reduction in the material mass during its pyrolysis is therefore a sum of contributions of $N_j$ reactions:

$$\frac{d\alpha}{dt} = -\sum_{j=1}^{N_j} A_j \alpha^{N_j} e^{-\frac{E_j}{RT}} \quad (1)$$

Here, $\alpha$ is the ratio of the current mass of the material with respect to its initial mass, $T$ and $R$ are material temperature and the universal gas constant (8.31431 J/K·mol) and , and are the elements of the so-called triplet of the kinetic parameters of the $j^{th}$ reaction ( is the pre-exponential factor in unit $s-1$, is the activation energy in unit kJ/k·mol, and is the reaction order). Note that , and are considered as constants and are usually not measured by laboratory tests but are instead defined via numerical fitting of Eq. (1) to results of TGA (Thermogravimetric Analysis) experiments (see e.g. [10-13]). The fitting is normally done using genetic algorithms or similar optimization methods. Results of TGA experiments that are used here should not only correspond to one fixed but rather to several different heating rates so that the finally defined (constant-value) kinetic parameters will correspond well (i.e. within tolerable limits) to different heating regimes to which the material may be exposed in a real fire.

Secondly, the classic Fourier equation of heat conduction in non-porous solids is used in FDS [10] to describe material pyrolysis:

$$\rho c_p \frac{dT}{dt} = \frac{\partial}{\partial x} k \frac{\partial T}{\partial x} + \dot{q}_{s''} \quad (2)$$

Here, $\alpha$ is the ratio of the current mass of the material with respect to its initial mass, $T$ and $R$ are material temperature and the universal gas constant (8.31431 J/K·mol) and , and are the elements of the so-called triplet of the kinetic parameters of the $j^{th}$ reaction ( is the pre-exponential factor in unit $s-1$, is the activation energy in unit kJ/k·mol, and is the reaction order). Note that , and are considered as constants and are usually not measured by laboratory tests but are instead defined via numerical fitting of Eq. (1) to results of TGA (Thermogravimetric Analysis) experiments (see e.g. [10-13]). The fitting is normally done using genetic algorithms or similar optimization methods. Results of TGA experiments that are used here should not only correspond to one fixed but rather to several different heating rates so that the finally defined (constant-value) kinetic parameters will correspond well (i.e. within tolerable limits) to different heating regimes to which the material may be exposed in a real fire.

Secondly, the classic Fourier equation of heat conduction in non-porous solids is used in FDS [10] to describe material pyrolysis. Here $X$ is the direction of heat transfer and $\dot{q}_{s}''$, $\rho$, $c_p$, $k$ are the constants representing the internal heat source (i.e. heat of the $N_j$ internal reactions) and the triplet of the material thermal parameters (density, specific heat, thermal conductivity). Although in this case measuring $\dot{q}_{s}''$, $\rho$, $c_p$, $k$ would normally be feasible with relatively simple material experiments (at least for normal ambient temperature conditions), these parameters too are to be determined via a specifically designed numerical fitting where the results of the pyrolysis model, governed by Eqs. (1) and (2), are to be fitted to the results of cone calorimeter experiments (see e.g. [10, 11]). Also in this case, a fixed set of the parameter values is to be defined to correspond within tolerable limits to different possible circumstances of material burning. Thus, results of several cone calorimeter tests performed at different heat fluxes of the cone radiator should be used in the process instead of the result of a single test.

As explained before $A_j$, $E_j$, $N_j$ and $\dot{q}_{s}''$, $\rho$, $c_p$, $k$ are to be defined through a numerical fit of the FDS pyrolysis model (governed by the Arrhenius and the classic Fourier equation) first to results of TGA experiments and later to results of cone calorimeter tests. As proposed in [10, 11], during such fitting, the applied fitting tool (e.g. genetic algorithm) should call FDS for creating TGA and cone calorimeter test simulations. Although at least for fitting the TGA data, it would be easier to simply solve the Arrhenius equation without the simulator, using it makes sure that the solution is applicable to FDS for later use. At the same time, this also means, that the values of the determined kinetic and thermal parameters might be FDS-version specific (note that the general form of FDS equations invoked by a TGA and/or a cone calorimeter simulation can reform over the FDS versions).

**Combustion model**

The combustion model defines the equation of chemical reaction in the gaseous phase, i.e. the reaction of fuel, vapor, and oxygen (stoichiometric equation). Two possible ways of such definition are available in FDS [10], i.e. simpler mixture fraction model and the more complex finite rate combustion model. For purposes of this paper the former was used. As stated in [10], using the mixture fraction model, the reaction is assumed to be of the form:

$$C_xH_yO_zN_v + n_{O_2}O_2 \rightarrow n_{CO_2}CO_2 + n_{H_2O}H_2O + n_{CO}CO + n_S soot + n_{N_2}N_2 \quad (3)$$

The FDS user only needs to specify the chemical formula of the fuel along with the yields of CO, soot, and $H_2$, and the amount of hydrogen in the soot. For some of the most typical chemical reactions, the corresponding values can be found in the literature (e.g. in [14]). For completeness, the $N_2$ content of the fuel and the presence of other species can be defined as well. FDS will use that information internally to calculate the amount of combustion products that are formed.

**FDS simulation of the 2016 fire in Jesenice**

An advanced computer reproduction of the 2016 Jesenice fire was developed by Kolšek [3] and this was used as the basis also in this paper (note that the details of the model of Kolšek [3] were presented later also in [15]). In the model of Kolšek [3], the calculation domain was defined in a 3D coordinate system following the main geometrical features of the fire-affected part of the building (Figure 1) where appropriate extensions of the domain were added in all three directions to minimise possible undesirable effects of the mesh boundaries. An OPEN VENT was placed over the entire top of the computational domain for the inflow of fresh outside air and the extraction of smoke. The thermal properties (density, thermal conductivity, specific heat capacity) of the outer RC walls and the RC ceiling (all of thickness 20 cm) were set as suggested in EN 1992-1-2:2004 [1] and the backing of these surfaces was set as EXPOSED following instructions of [10]. The openings in the walls, i.e. windows and doors, were modelled using the HOLE feature. In addition, the parameters for PMMA material (polymethyl methacrylate) as derived in the master thesis of Matala [11] were used for the pyrolysis modelling of the material of the tyres considering relevant similarities of PMMA and car tire burning, [16-18]; (further argumentation for this choice is given in [3, 15]). As already explained earlier, during the fitting of the material pyrolysis parameters, the applied fitting tool normally calls FDS for creating TGA and cone calorimeter test simulations and this was also the case in [11]. Using the FDS in this process makes sure that the solution is applicable to FDS for later use, but it also means that the determined values of the parameters might be FDS-version specific. Thus, the same version of FDS as used in [11] was used in the analyses of [3, 15] and also the analyses of this paper. The thickness of all tires (combustible layers only) was considered as 0.04 m. In contrast to the detailed pyrolysis modelling of the tyre burning, however, only the simpler mixture fraction model was set for describing the chemical reaction in the gas phase, as proposed in [3, 15]. This was because the goal of our FDS modelling was calculating the temperatures of the affected fire compartment, but detailed analysis of the production and the transport of gaseous species was not our focus. Furthermore, the FDS simulation was performed using a single uniform mesh with a cell size of 20 × 20 × 20 cm. Such a mesh might appear somewhat coarse, but it assures sufficient numerical efficiency of the model and, as shown in [3, 15], it also proves to be sufficient to obtain results of reasonable accuracy. In [[3, 15], this was demonstrated in the way that the Jesenice fire model, as briefly presented above, was first exploited for calculating the maximum depth of the 500°C isotherm as it developed in the most-affected real Jesenice columns (i.e. round columns of 50 cm diameter). The results suggested this depth to be about 6 cm below the surface of the columns whereas the experimental results of the laboratory examination of the concrete samples, taken from these columns during their post-fire inspection, implied a 5-8 cm depth (note that the post-fire inspection was also reported on in [3, 4].

Finally, to fully follow the goals of the present paper, the model of Kolšek in [3] as described above was upgraded slightly. While in the original model the RC columns of the affected part of the basement (i.e. columns S1-S13 in Figure 1) were not modelled specifically, these were added as additional solid obstructions in the model of the present paper. The reason was that one of the effects to be tested later in the paper was also the effect of the convective heat transfer coefficient (CHTC) but the FDS device dedicated to measurement of CHTC could only be attached to a solid surface. Namely, the value of CHTC in general not only depends on the temperature of the gas but also on the velocity of the gas flow and the type of the gas movement (laminar or turbulent), both depending on the properties of the surface. The obstructions representing columns S1-S13 were in FDS [10] modelled in the way that each side of each column was modelled with a 10 cm thick surface provided with an INSULATED backing and suitable thermal properties of the concrete as suggested in [1]. Four HEAT TRANSFER COEFFICIENT devices were placed on the surface of each column at a height of 2.5 m, i.e. 30 cm below the basement ceiling (one on each of the four sides). The CHTC curve, representing the time-change of CHTC to be exported for later use in step 2 of the procedure, was then calculated as the average of the four measurements. In addition, the ADIABATIC SURFACE TEMPERATURE (AST) devices were also installed at the same positions and their results were later averaged in the same manner. The averaged AST result was then used later for the definition of the fire curve of step 2 of the procedure.

In step 2 of the procedure, which will be described in the following section of the paper, the temperatures of concrete across the volume of the RC column will be calculated by the classical Fourier equation where convective and radiative heat transfer at the solid boundary will depend on the fire curve. The fire curve will represent the temperature of the surroundings of the structure to which this is exposed during the fire. The term "surroundings" here refers, firstly, to the surrounding gas, which exchanges heat with the analyzed structure via convection, and, secondly, to the temperature of the surrounding flame, walls and other obstructions in the fire compartment that swap heat by radiation. Obviously, by applying a fire curve, which is a function that only depends on time but not also on space, we assume that the temperature of all these components (gas, flame, walls and other obstructions within the fire compartment) is essentially the same or very similar. Depending on the specifics of the analyzed case and the current time of the fire, however, the latter might not always hold true exactly. Thus, the temperature of the fire curve must be considered a fictitious rather than a real temperature. In FDS [10], this fictitious temperature is called ADIABATIC SURFACE TEMPERATURE (AST). AST is calculated in the way that the net convective and the radiative heat flux at the solid boundary as calculated from the CFD and radiation models in FDS is equal to the equation that is used later in step 2 of the procedure:

$$\dot{q}_r'' + \dot{q}_c'' = \varepsilon\sigma(T_{AST}^4 - T_c^4) + h(T_{AST} - T_c) \quad (4)$$

In Eq. (4) the sum on the left side of the equation is the sum of radiative and convective heat fluxes entering the solid boundary (i.e. the outer surface of the observed column) and the denotations $T_c$, $\varepsilon$, and h, on the right side represent the properties of the boundary (i.e. the temperature of the column's surface, the radiation coefficient, and the convective heat transfer coefficient, respectively). $T_{AST}$ is the temperature of the column's surrounding and $\varepsilon$ is the Stefan-Boltzman constant.

### 2.3.2. Thermal analysis of the column (step 2)

The model for the calculation of time-dependent temperatures of column S2 was set up in ABAQUS [19] as a standard Fourier analysis of non-stationary heat transfer through non-porous solids. A mesh density of 0.01 x 0.01 x 0.01 [m] and linear solid finite elements of type DC3D8 were used for concrete. Steel rebars were discretised by DC1D2 truss finite elements. The fire curve was defined using the results of the previous first step of the analysis. If in the latter a nominal fire curve was selected, the convective heat transfer coefficient (abbreviation CHTC will be used further) was assumed to be 25 W/m$^2$K [2]. If a natural fire curve exported from FDS [10] was considered, the CHTC was assumed to be 35 W/m$^2$K or the values for CHTC were also imported from the FDS model. Following the suggestion of [1], the radiation coefficient of the concrete surface was set at 0.7 in all analyses. In addition, the densities of the concrete and the rebars were assumed to be constant (i.e. 2500 kg/m$^3$ and 7850 kg/m$^3$, respectively), but their thermal conductivity and specific heat capacity were considered to be temperature-dependent and were set as proposed in [1]. Concrete with 2% moisture was considered in the definition of the heat capacity of the concrete. In most cases studied in this paper, only one fire curve was applied along the entire height of the column, but in some cases two or more typical regions (thermal zones) were defined as well for comparison. The latter considered the fact that in real building fires the air temperatures below the ceiling are higher than those at the ground (warmer air rises due to buoyancy and cooler air moves downwards).

### 2.3.3. Mechanical analysis of the column (step 3)

In a fire, an RC column essentially collapses because of one of two possible reasons: (i) loss of the load-bearing capacity of the cross-section or (ii) buckling of the column and consequent loss of its stability. However, which of the two possibilities of collapse occurs first, depends on the slenderness of the column. The latter changes over time as an indirect consequence of high concrete temperatures, which lead, for example, to a gradual reduction in material strength in the outer (hotter) layers of the column, delamination of these layers due to concrete spalling, etc.

In this paper, three selected calculation methods proposed by EN 1992-1-2:2004 [1] are used to assess the fire resistance

of the column – all considering both possible mechanisms of structural collapse (cross–sectional collapse or buckling). The first two methods are simplified methods that use a 2nd-order theory to account for the deformations of the column and consider the temperatures of the cross–section and the corresponding material strengths in a more (*Simplified procedure 2*) or less (*Simplified procedure 1*) exact manner. The third method is a more advanced method based not only on a detailed consideration of the material temperatures, but also on the description of the deformations of the column according to a more advanced materially and geometrically nonlinear theory.

**Simplified procedure 1**

This procedure is a representative of the so-called *reduced cross-section procedures* where the reduced area of the concrete part of the column's cross-section is to be determined first for the observed time of the fire under our consideration. This is done by the so-called 500°C isotherm method. The latter assumes that the strength and elastic modulus of concrete are fully preserved up to a concrete temperature of 500°C. But at temperatures above 500°C, the load capacity of concrete is lost entirely. After the reduced concrete cross-section (i.e. concrete area enclosed by the 500°C isotherm) is known, the load-bearing capacity of the column can be checked, e.g., by the method based on nominal curvature as known well from the basic design of slender RC columns at normal (room) temperature (see Section 5.8.8. of EN 1992-1-1:2004 [20]). Only the reduced part of concrete is considered here and this is assumed to preserve its initial material strength. Reinforcement bars, however, are considered with a reduced strength corresponding to the proposal of EN 1992-1-2:2004 [1] in dependence on their actual temperature.

**Simplified procedure 2**

This procedure is similar to simplified procedure 1 described above and it is based on provisions of Annex B.3 of EN 1992-1-2:2004 [1]. Instead of accounting only for concrete inside the 500°C isotherm, however, we now account for the entire concrete region. For each of its points, the actual temperature is first read from the results of the thermal analysis and then the corresponding first-order bending moment capacity of the column (corresponding to axial internal force ) is determined using a predefined M–κ relationship. The procedure is summarized in brief below:

- The Euler-Bernoulli hypothesis, which states that the cross-sections of a beam-like structural element remain undeformed and perpendicular to the longitudinal axis of the element at any point in time, is applied via the equation:

$$\varepsilon(y, z) = \varepsilon_0 + z \cdot \kappa \tag{5}$$

Here κ is considered as a known quantity but denoting the longitudinal strain of the column at the centroid of its cross-section is unknown. ε (*y, z*) is longitudinal strain in point (*y, z*) of the cross-section. This may refer to concrete or a reinforcing bar. An assumption is made that the reinforcing bar, being located at the position ($y_s$, $z_s$), and the surrounding concrete have equal strains, thus: $\varepsilon_c(y_s, z_s) = \varepsilon_s(y_s, z_s)$. In addition, at elevated temperatures, the longitudinal strain(*y, z*) is said to equal the sum of mechanical strains and thermal strains:

$$\varepsilon(y, z) = = \varepsilon_0 + z \cdot \kappa = \varepsilon_m(y, z) + \varepsilon_{th}(y, z) \tag{6}$$

According to EN 1992-1-2:2004 [1], thermal strains (y,z) are to be calculated as $\varepsilon_{th}(y, z)$**,** where is relative thermal expansion coefficient also given in [1].

- Secondly, Eq. (6) is inserted into the stress–mechanical strain relationships for concrete and reinforcing steel at elevated temperatures $\sigma_c(\varepsilon_{m,c})$ and $\sigma_a(\varepsilon_{m,a})$, as provided in [1].
- Thirdly, the relationships $\sigma_c(\varepsilon_{m,c})$ and $\sigma_s(\varepsilon_{m,s})$ are implemented in the known constitutive equation of beam-like structural elements, which defines that the axial force in the cross-section of the element is equal to the cross-sectional integral of the longitudinal normal stresses σ:

$$N = \int_A \sigma(y,z)dA = \int_{Ac} \sigma_c(y,z)dA_c + \int_{As} \sigma_s(y,z)dA_s \tag{7}$$

- Note that in Eq. (7) we account for the fact that the column's cross-section consists of two parts: the concrete part (section $A_c$) and the steel reinforcement (section $A_s$).
- The integrals of Eq. (7) are finally solved, e.g., in a simplified manner by dividing the concrete cross-section into smaller rectangular parts and accepting the assumption that in each point of a specific rectangle area the stress is equal to the stress in the centroid of this area. This simplifies Eq. (7) to the following form:

$$N = \int_A \sigma(y,z)dA = \sum_{A_{c,i}} \sigma_{c,i}A_{c,i} + \sum_{A_{s,j}} \sigma_{s,j}A_{s,j} \tag{8}$$

Here means the stress at the centroid of a rectangle part of the concrete section, $A_{c,i}$ is the surface of this part, $\sigma_{s,j}$ is the stress in the $j^{th}$ longitudinal reinforcing bar of the column, and $A_{s,j}$ is the corresponding cross-sectional area of this rebar.

- The actual value of the axial force can now be inserted in Eq. (8) ($N = N_{0,Ed}$) and the unknown can be derived.
- After this, the moment *M* corresponding to the initially selected value of $N = N_{0,Ed}$ can be obtained as well:

$$M = \int_A \sigma(y,z) \cdot z dA = \sum_{A_{c,i}} \sigma_{c,i}z_{c,i}A_{c,i} + \sum_{A_{s,j}} \sigma_{s,j}z_{s,j}A_{s,j} \tag{9}$$

Here $z_{c,i}$ and $z_{s,j}$ are coordinates of the centroid of a concrete part of the cross-section and of a reinforcing bar.

- In the derived *M*–κ curve, the maximum value of *M* is the bending resistance of the column in its deformed configuration (i.e. ). As such, the derived *M* is not yet eligible for a comparison towards because was calculated considering equilibrium of forces on the undeformed column's configuration. An $M_0$–κ curve should, thus, be derived as well, e.g., as suggested in [20]:

$$M_0 = M - M_2 \quad (10)$$

In Eq. (10) $M$ is the second-order theory bending moment referring to a specific curvature κ and $M_0$ is the corresponding first-order theory moment. Furthermore, $M_2$ is the nominal second-order moment defined as:

$$M_2 = N_{0,Ed} e_2 \quad (11)$$

where:

$$e_2 = \frac{1}{r} l_0^2 \frac{1}{c} \quad (12)$$

Here  is the curvature of the column (= κ,  is its buckling length (calculated according to EN 1992-1-1 [20], section 5.8.3.2) and c is coefficient of the value c ≈ 10.
Finally, the ultimate first order moment capacity of the column $M_{Rd0}$ can be read from the $M_0$-κ curve corresponding to $M_0$ where  is reaching its maximum (i.e. the value of  right at the point when this curve takes a downward turn).

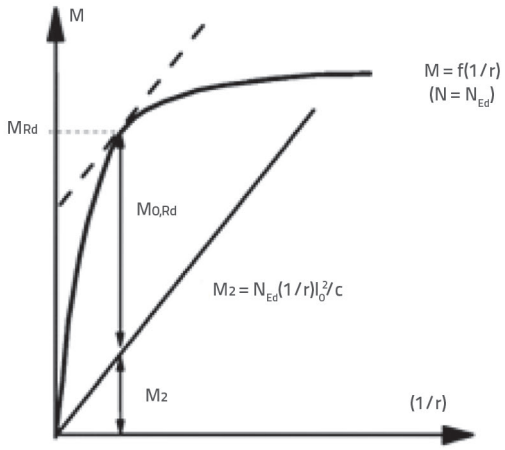


**Figure 4. Schematic presentation of determination of the ultimate second-order and the ultimate first-order moment capacity of the column ($M_{Rd}$ and $M_{0,Rd}$) as suggested in [1]**

$M_{0,Ed}$ and $M_{0,Rd}$ can now be compared:
a) $M_{0,Ed} < M_{0,Rd} \rightarrow$ the column withstands the assumed fire,
b) $M_{0,Ed} > M_{0,Rd} \rightarrow$ the column cannot withstand the assumed fire.

**Advanced procedure**
The advanced procedure used in this paper is based on the equations of the geometrically and materially nonlinear theory of solid body mechanics at high temperatures. This model was created in ABAQUS [19] wherein the basic geometric features were first imported from the Abaqus model of step 2. The column was then discretized using finite elements of type C3D8 for concrete and truss finite elements of type T3D2 for steel rebars. The same mesh density was used as in the thermal model (i.e. 0.01 x 0.01 x 0.01 [m]). Next, appropriate kinematic boundary conditions were applied. At the lower end, the rotations and displacements of all nodes were set to zero, while at the upper end, the horizontal displacements of all nodes were prevented by constraining the horizontal displacements of one node (the so-called reference point, which coincided with the center of the column) and additionally applying a rigid body constraint to the remaining nodes of the cross-section. The concentric axial force of 1000 kN was applied at the top of the column. In order to indirectly induce the effect of a geometric imperfection of the column, a small transverse load was added to the model at the mid-height of the column. The corresponding maximal bending moment induced in the column in this way was $M_{0,Ed}$ = 0.285 kNm. In terms of the relevant material properties of the concrete, constant densities of 2500 kg/m³ and 7850 kg/m³ were applied again for concrete and reinforcing steel, while for the temperature-dependent expansion coefficient and the stress-strain relationship of these two materials, the proposals of EN 1992-1-2:2004 [1] were used.

## 2.4. Study of the effect of different modelling choices on the calculated fire resistance of column S2

### 2.4.1. Model 0 (the reference model)

*Model 0* is considered as the reference model of the paper. In step 1, the FDS model as proposed in Section 2.3.1 is used. The AST temperatures and values of CHTC are exported from this step for column S2 at the height of 2.5 m above the ground level for the definition of the fire– and the CHTC curve to be used in the following step. Step 2 is then performed in Abaqus as described in Section 2.3.2. After completion of step 2, the results of the thermal analysis are imported as temperature fields into the corresponding model of step 3 (i.e. fire resistance model). Here the column is analysed using the *advanced procedure* as described in Section 2.3.3.

### 2.4.2. Model 1: exploring the influence of CHTC

Instead of using the FDS-exported values for CHTC as in the case of *Model 0*, the proposition of EN 1991-1-2:2002 [2] is followed and the constant value of 35 W/m²K is applied in step 2 of *Model 1*. All other features of the model are the same as in *Model 0*.

### 2.4.3. Model 2: exploring the effect of the procedure of step 3)

The purpose of *Model 2* is to further explore the implications of the chosen mathematical description of the structural response of the column as applied in Step 3. The features of steps 1 and 2 are in this model taken as in *Model 0*. However, two simplified 2nd-order theory models are tried out for step

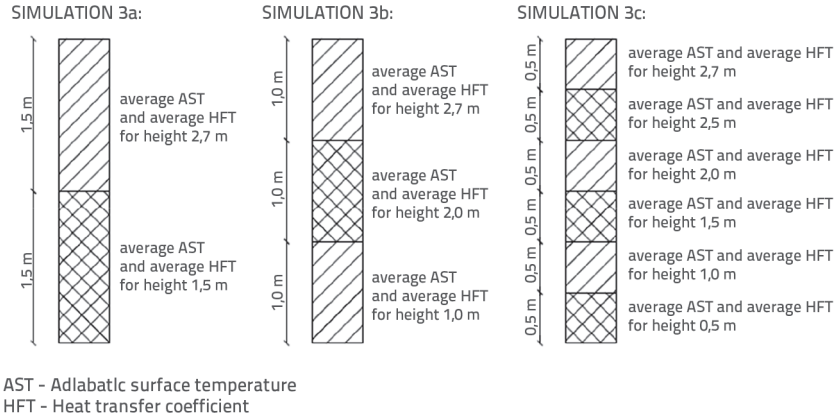


**Figure 5. Heat zones in Models 3a (left), 3b (middle) and 3c (right)**

3 as described in Section 2.3.3, i.e. *Simplified procedure 1* (*Model 2a*) and *Simplified procedure 2* (*Model 2b*). In both cases (*Model 2a* and *2b*), the structural analysis of the column is to be repeated at different times of the fire until the time of collapse of column S2 is found at the time when $M_{0,Ed}$ is equal to $M_{0,Rd}$.

### 2.4.4. Model 3: exploring the effect of the number of heat zones

In *Model 0,* only one fire curve was applied along the entire height of the column but two (*Model 3a*), three (*Model 3b*) or six (*Model 3c*) such curves are used in the group of *Models 3* representing the temperature of the column's surrounding in two, three, or six different heat zones (in what follows, abbreviation HZ will be used). In the same way, the values of CHTC are also applied. The selected HZ extend along the column's height and are of equal heights (Figure 5).

For each zone, the magnitude of AST or CHTC at a height *Z* above the ground level and at a specific time *t* of the fire is taken as the average of the output of the four corresponding FDS devices (i.e. AST or HFT devices), each of the latter being installed on one of the four surfaces of the column and at the specific height Z.

Except for accounting for different heat zones as explained above, no other changes are applied in steps 1 and 2 of the group of *Models 3* compared to *Model 0.* The procedure of step 3 of *Models 3* is identical to that in *Model 0.*

### 2.4.5. Model 4: exploring the effect of the variability of the axial load

In the simplified member-analysis methods for assessing the fire resistance of concrete columns according to EN 1992-1-2:2004 [1] the column is to be evaluated under a constant mechanical load that remains equal to the initial load $N_{0,Ed}$ (i.e. the load at the start of the fire). However, it is now known (e.g., [21, 22]) that in real fires in RC structures, the loads on an RC column can change with time, mainly at the expense of hindered temperature deformations in the earlier stages of the fire and the gradual reduction of the stiffness of the column and the redistribution of the loads to the neighbouring part of the structure in the later stages (when the column approaches its fire resistance). However, there is a lack of tangible data in the literature on how much such an approximation can influence the result of the calculation. For the particular case analysed in this paper, this question is to be explored in the scope of *Model 4*.

An accurate calculation of the influence of the variability of the axial load on column S2 would require additional modelling of the entire structural system of the affected part of the basement which, however, is not the subject of this paper. Thus, only approximate estimates of the variability of the axial force in column S2 are used based on the data from relevant literature. Considering the conclusions of Mostafei [21] and Tadić [22], the fire-induced changes in the internal forces of a column of an RC frame building will be governed greatly by the way the neighbouring structure will be heated compared to the heating regime of the column itself. In addition, as it seems, at least a 10% maximum increase should be expected for the axial force. Thus, two courses of changes in the axial force were considered as realistically possible for column S2 analysed in this paper, see Figure 6. A more precise evaluations of these effects are planned for later works of the authors.

The procedures of steps 1 and 2 of *Models 4a* and *4b* were identical to those in *Model 0.* The procedure of step 3 was also identical with the exception referring to the axial load applied on the top of the column. Contrary to *Model 0*, this did not remain constant at 1000 kN at all times, but followed the course presented in Figure 6.

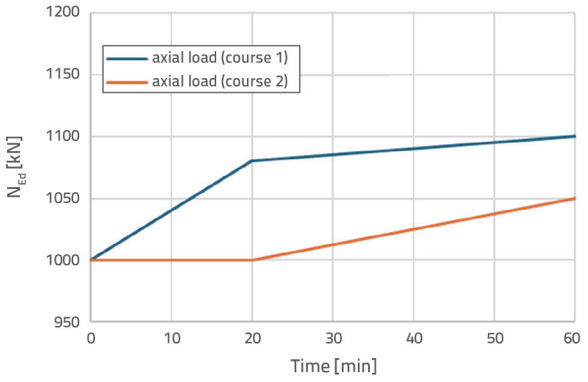


**Figure 6. Two courses of the column's axial load as applied in Models 4a and 4b**

### 2.4.6. Model 5: exploring the effect of the selection of the fire curve

Model 5 finally explores the effect of the selection of the fire curve. Instead of the natural fire curve, as so far embedded into the first step of all previous models, this time the standard fire curve as suggested in EN 1991-1-2:2002 [2] is applied. In practical engineering, the latter undoubtedly represents the mostly applied normalised fire curve. Every other feature of steps 1-3 of the procedure remains unchanged compared to *Model 0*.

## 3. Results and discussion

### 3.1. Results of the FDS analyses – Step 1

Figure 7 below shows the average AST temperature for column S2 resulting from our FDS calculations as described above (the red curve). For comparison, the graph of gas temperatures, measured at the same location, is added as well (the blue curve). While both graphs seem similar in their general course, the magnitudes of the temperatures shown reveal some differences in specific regions.

Furthermore, a graph of corresponding gas temperatures as calculated using the original model of Kolšek [3] is also shown in the same figure (the black curve). Some differences can be noticed here in the general course of the curve as well as in the achieved temperature magnitudes compared to gas temperatures of the present model. This implies some numerical sensitivity of the composed fire-growth model (recall that the only difference between the original and the present model was whether columns S1-S13 were put as additional physical obstructions in the model). This will be taken into consideration later in the preparation of the main conclusions of the paper.

Figure 8 shows the comparison between the natural fire curves, calculated using the present FDS model and applied in models 0-4, and the standard fire curve used in model 5.

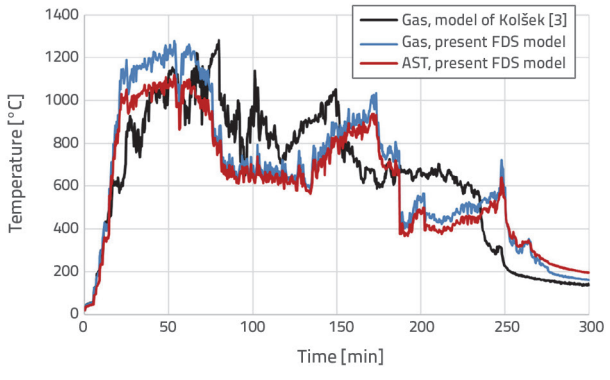


**Figure 7. Average gas temperature (blue curve) and average AST temperature (red curve) for column S2 at a height of 2.5 m above the ground level as calculated with the present FDS model. For comparison, gas temperatures at the same location are also shown as calculated with the original model of Kolšek [3] (thick black line)**

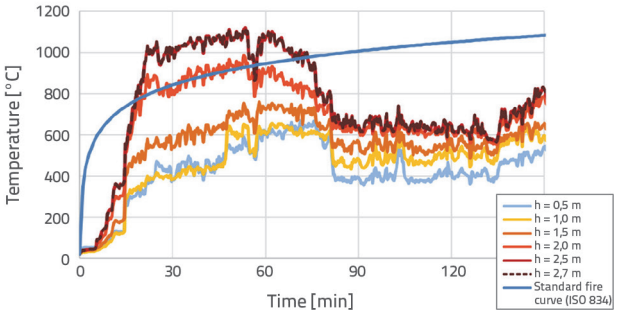


**Figure 8. Adiabatic surface temperatures (AST) for column S2 at different heights above the ground level (calculated with the present FDS model) compared to Standard fire curve**

Furthermore, Figure 9 also shows the results of the present FDS model for the time-dependent values of CHTC. The values here seem to differ significantly compared to the constant value of 35 W/m$^2$K which is suggested to be used in combination with a natural fire curve in EN 1991-1-2:2002 [2].

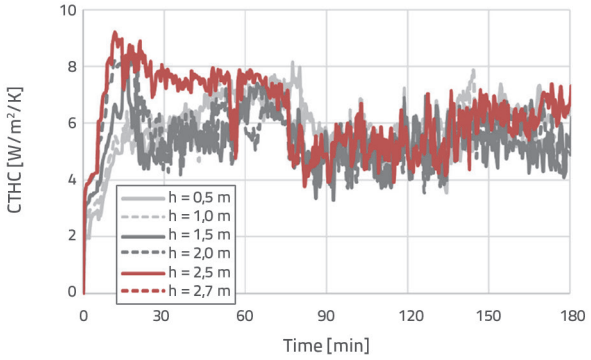


**Figure 9. Convective heat transfer coefficient (CHTC) for column S2 at different heights above the ground level (calculated with the present FDS model)**

### 3.2. Results of the thermal analyses – Step 2

Figure 10 presents the evolution of temperatures for models using only one heat zone at two points of a cross-section of the column at mid-height. Point $T_R$ is located at the side reinforcement bar, and point $T_C$ is at the center of the cross-section (see Figure 2). It can be observed that the courses of the curves are similar to each other; therefore, it is not expected that the selection of the fire curve and CHTC will greatly affect the results of the mechanical analysis.

Furthermore Figure 11 presents the evolution of temperatures at points $T_R$ and $T_C$ for models 3a, 3b, and 3c, where the effect of different numbers of heat zones is studied. For model 3a, the temperatures are presented in cross-sections at the mid-heights of the two zones; for model 3b, at the mid-heights of the three zones; and for model 3c, at the mid-heights of the six zones. It can be observed that the bottom part of the column remains significantly cooler than the upper part; therefore, it is

expected that dividing the column into more than one heat zone will affect the results of the mechanical analysis.

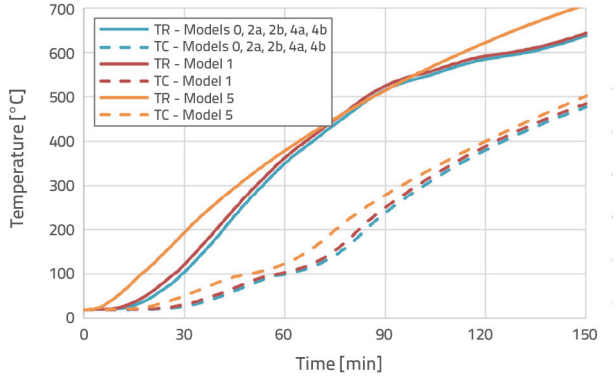


**Figure 10. Temperature evolution at reinforcement point $T_R$ and column center $T_C$ for Models 0, 1, 2a, 2b, 4a, 4b, and 5**

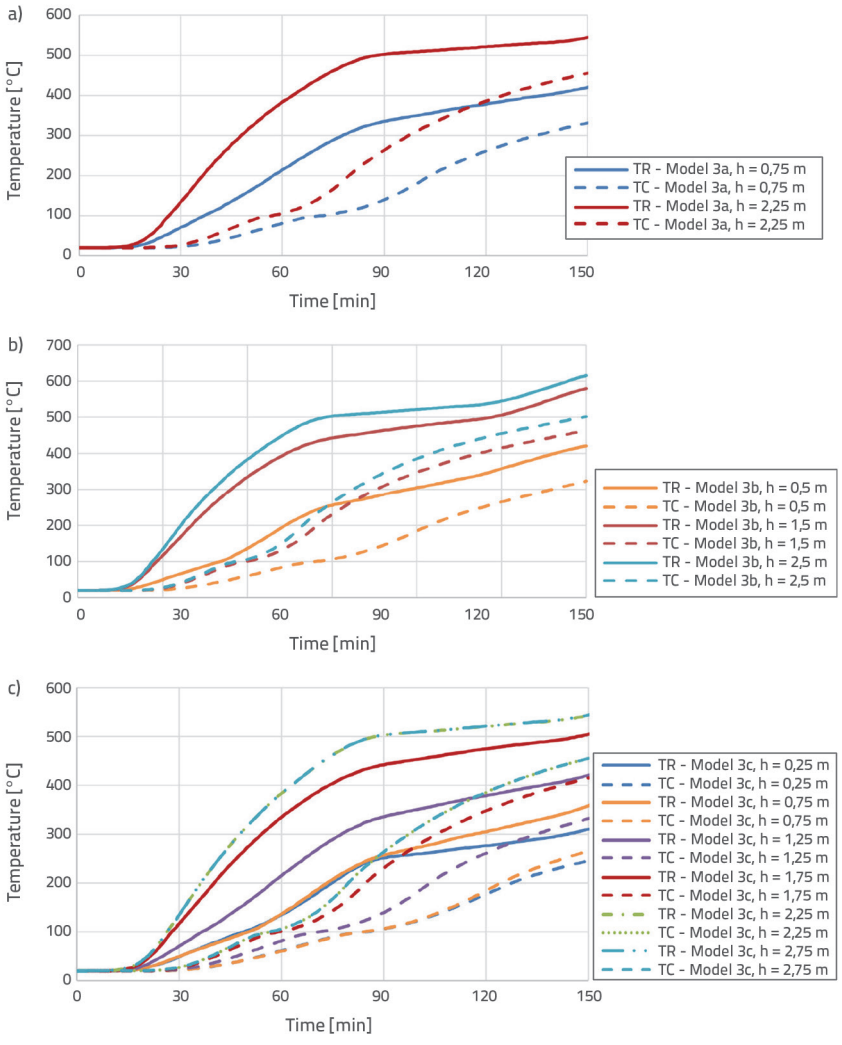


**Figure 11. Temperature evolution at reinforcement point TR and at column center TC for models: a) Model 3a; b) Model 3b; c) Model 3c**

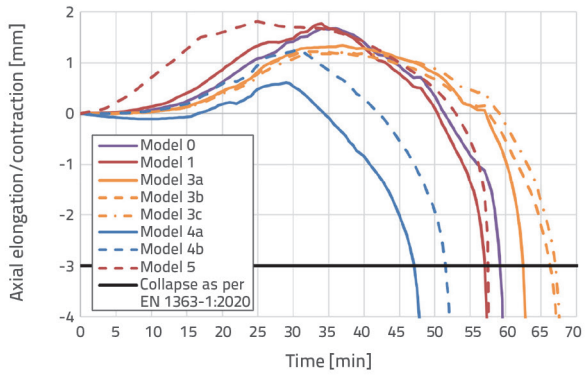


**Figure 12. The time development of the axial displacement (elongation/contraction) of the top of the column**

### 3.3. Results of the mechanical analyses

In standardized fire testing, the EN 1363-1:2020 [8] standard is normally used for obtaining general guidelines and requirements for the fire resistance of load-bearing structures. Among others, this standard also deals with load-bearing columns (including RC columns), where considering the latter specific limits are given for the magnitude and the rate of the vertical contraction of the column at which the test should be terminated and the fire resistance of the column should be declared to be achieved. This general idea was analogously followed in the groups of *Models 0, 1* and *3-5* to determine the time of collapse. Figure 12 illustrates the vertical displacement graphs of the column's top, as calculated in Models 0, 1, and 3-5, plotted against the maximum contraction: , as defined in EN 1363-1:2020 [8].

In the group of *Models 2*, however, a different description of the mechanical response of the column was used in Step 3 compared to the other models and no calculation of the column deflections was performed. For this reason, the fire resistance of the column was defined differently in these cases, i.e. as the time of the fire when the initial bending moment of the column $M_{0,Ed}$ was equal to $M_{0,Rd}$ considering the predefined M–κrelationship (see Section 2.3.3). Figure 13 and Figure 14 present the M–κ relationships for *Models 2a* and *2b* for the time when $M_{0,Ed}$ equals $M_{0,Rd}$ in the model, i.e. 40 min (*Model 2a*) and 45 min (*Model 2b*).

**Table 1. Collapse times for all models**

| Model | 0 | 1 | 2a | 2b | 3a | 3b | 3c | 4a | 4b | 5 |
|---|---|---|---|---|---|---|---|---|---|---|
| $t_{slom}$ [min] | 59 | 57 | 40 | 45 | 62 | 66 | 67 | 47 | 51 | 57 |

The results for the time to collapse (denoted as $t_{collapse}$) of column S2 calculated as explained above, are summarized in Table 1.

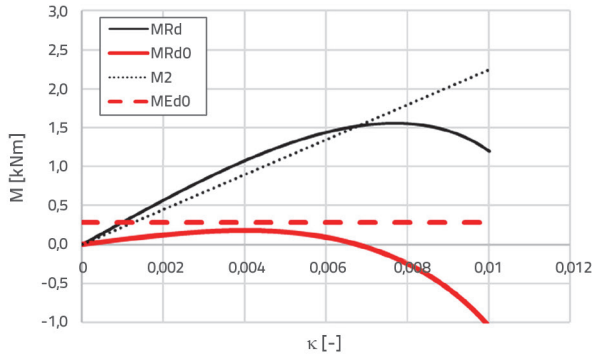


**Figure 13. Model 2a: M-κ curves for t = 40 minutes.**

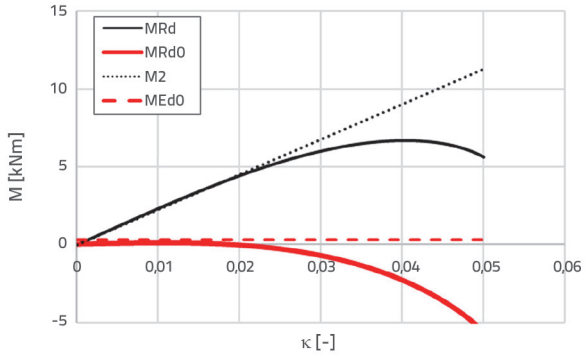


**Figure 14. Model 2b: M-κ curves for t = 45 minutes**

### 3.4. Discussion

Table 2 below firstly summarizes the basic features of each of the three steps of the above discussed models (see columns 2-4). For step 1, the type of the fire curve to be defined in step 1 is provided first (natural or nominal) along with the source of its definition, i.e. FDS [10] or EC1 [2]. In addition, the number of heat zones (HZ) that are accounted for along the height of the column is given. Furthermore, for step 2, the source of the imported fire curve(s) and convective heat transfer coefficient(s) are given (FDS [10] or EC1 [2]) and the number of heat zones (HZ) considered is again noted. Finally, the main data of step 3 is also provided. The latter refer to the type of the procedure used (one of the three procedures described in Section 2.3.3) and the type of the axial force applied on the top of the column (constant or variable). Additional specification is given in brackets for variable type load which refer to one of the two inspected axial load courses (Figure 6).

A comparison of the fundamental result of each model, i.e. time to collapse of column S2 ($t_{collapse}$), to the corresponding result of the reference *Model 0* finally enables assessment of the investigated effects of individual analysis parameters. A short summary of the comparison is given in the last four columns of Table 2. In the analyses, where the preciseness of the description of the analysed problem was increased on account of the applied changes, an "↑" sign is added in the sixth column along with the information on the investigated parameter. In contrary, a "↓" is used if the analysis preciseness was reduced. Obviously, following the common engineering principles, a reduction of the analysis preciseness should reflect in a result that is on the "safe-side" compared to the result of the more precise models. Unfortunately, however, this does not prove to be always true in our case (see the last column of Table 2).

In the seventh column of Table 2 the discrepancies between the observed *Models 1-5* compared to reference *Model 0* are also given in percentages. *Model 1* does not show an obvious discrepancy here compared to *Model 0*. Recall that in *Model 0* the more reliably assessed time-dependent values for
CHTC were used as exported from the FDS model but a simplified constant value was applied for this coefficient in *Model 1* following the proposition of EN 1991-1-2:2002 [2]. This shows that the effect of two possible selections of the values for CHTC only is minor in our case. The conclusion might appear unexpected at first glance considering the large differences in magnitudes of CHTC that were applied in these two models. Nevertheless, large differences in the values of CHTC would not necessarily also mean large differences in the calculated cross-sectional temperatures because the influence of radiation will predominate (recall that the temperatures of the surroundings of the column are raised to the fourth power in the calculation of radiative heat fluxes, see Eq. (4)).

A larger discrepancy (i.e. 24-32%), however, is observed between *Model 0* and the group of *Models 2.* The latter shows that the degree of conservatism introduced into the analysis, when a geometrically nonlinear description of the structural response is replaced by a simpler 2$^{nd}$-order theory in step 3, is in fact noticeable for the analysed building and fire case. Nevertheless, a firm "safe-side" is proved for the 2$^{nd}$-order theory approximations.

Moreover, by further investigating the effect of considering two heat zones extending along the height of the column (e.g. an upper hotter zone and a lower colder zone) (*Model 3a*) instead of just one zone (*Model 0*) and consideration of two different fire– and CHTC curves for each of the two, a minor change between the results of the compared models is found again. The time to collapse of the observed column increases by 5% in this case and this points to a "safe-side" approximation if only one heat zone is considered in the model. A more pronounced increase in the time to the column's collapse is further observed when the

**Table 2. Summary of the main features and the results of the composed models**

| Model | Fire analysis | | | $t_{collapse}$ [min] | Parameter tested (change in preciseness of the analysis) | Change in $t_{collapse}$ [min/%] | Use of simplification: safe / unsafe *** |
|---|---|---|---|---|---|---|---|
| | Step 1: Type of fire curve, Source of its definition (number of HZ) | Step 2: Source of the fire curve, CTHC (number of HZ) | Step 3: Type of the procedure, Type of the axial force | | | | |
| 0 | Natural, FDS (1) | FDS, FDS (1) | Advanced, constant | 59 | - | - | - |
| 1 | Natural, FDS (1) | FDS, EC 1 (35 W/m²K) (1) | Advanced, constant | 57 | CTHC (↓) | –2 / –3% | safe |
| 2a | Natural, FDS (1) | FDS, FDS (1) | Simplified 1, Constant | 40 | Procedure of Step 3 (↓) | –19 / –32% | safe |
| 2b | Natural, FDS (1) | FDS, FDS (1) | Simplified 2, Constant | 45 | Procedure of Step 3 (↓) | –14 / –24% | safe |
| 3a | Natural, FDS (2) | FDS, FDS (2) | Advanced, constant | 62 | Number of HZ (↑) | +3 / +5% | safe |
| 3b | Natural, FDS (3) | FDS, FDS (3) | Advanced, constant | 66 | Number of HZ (↑) | +7 / +12%* | safe |
| 3c | Natural, FDS (6) | FDS, FDS (6) | Advanced, constant | 67 | Number of HZ (↑) | +8 / +14 %** | safe |
| 4a | Natural, FDS (1) | FDS, FDS (1) | Advanced, Variable (tip 1) | 47 | Variability of axial load (↑) | –12 / –20 % | unsafe |
| 4b | Natural, FDS (1) | FDS, FDS (1) | Advanced, Variable (tip 2) | 51 | Variability of axial load (↑) | –8 / –14 % | unsafe |
| 5 | Nominal (standard), EC1 (1) | EC 1, EC 1 (25 W/m²K) (1) | Advanced, constant | 57 | Fire curve (↓) | -2 / -3 % | not determined |

* +6 % compared to Model 3a.
** +1.5 % increase compared to Model 3b.
*** Safe: The assumptions made for the model underestimate the fire resistance of the column.
Unsafe: The assumptions made for the model overestimate the fire resistance of the column.

number of zones increases additionally, i.e. from two (*Model 3a*) to three (*Model 3b*) and to six (Model 3c) zones. Here, the time to collapse of the observed column increases by 12% and 14% respectively.

The comparison of the results of *Models 4* and *Model* 0 shows the effect of accounting for the variability of the axial force applied on the top of column S2. Although the reliability of the analysis results should increase in such models given the greater accuracy of the axial force, this (as expected) does not prove to be true for the analysed case. This shows that neglecting the effect of the restrained thermal elongation of the column, which is in real building fires normally expected because of the neighbouring structure, is in fact unsafe.

The comparison of the results of *Model 5* to the results of *Model 0* finally reveals the effect of potential engineering decision on using the simplified standard fire curve from EN 1991-1-2:2002 [2] instead of following the advanced CFD-based natural fire curve. The results of both models are rather similar which is expected since the general course of the FDS curve and the general course of the standard fire curve are not very different up until the time of the column's failure. The FDS curve indeed predicts somewhat higher temperatures from the 20th to 30th minute of the fire, but it also shows considerably lower temperatures prior to the 20th minute. Nevertheless, a 3% decrease in $t_{collapse}$ is observed after the implementation of the standard curve. The latter conclusion is "safe", but considering the numerical sensitivity of the fire-growth model standing behind the FDS analysis , the observed 3% discrepancy is too low to reliably support this conclusion (recall the results of Figure 7 and the corresponding discussion on comparison of the gas temperatures exported from the model of Kolšek [3] and the present FDS model).

### 3.5. Comments on the applicability of the collected findings

It is the authors' belief that, even if columns of a larger cross-section (i.e. a more common size of the cross-section as seen in real buildings) were selected for the parametric study of this paper, this would not affect the general conclusions of the paper. In this case, the columns would not collapse in our analyses, thus, the comparison between the calculated times to collapse would not be. However, a comparison between the after-fire load-bearing capacity of the column would still be possible and this would reflect similar findings.

## 4. Conclusions

This study systematically examined the impact of different modelling choices on the fire resistance of RC columns according to EN 1992-1-2:2004 [20], using a real-world case study. The investigation was performed on a selected RC building and a real fire that broke out in this building in late 2016. Simplifications in thermal and structural analyses can reduce computational effort and design costs, but their safety must be carefully evaluated.

The methodology involved a comparative analysis of multiple modelling approaches, ranging from simplified methods to advanced numerical simulations. Specifically, the study employed the Fire Dynamics Simulator (FDS) for generating natural fire curves and ABAQUS for thermal and mechanical analyses. The fire analysis was divided into three essential steps: determination of the temperature of the column's surroundings (fire scenario), thermal analysis of the column, and mechanical analysis up to failure.

The results highlighted how specific assumptions affect key performance indicators such as load-bearing capacity and fire resistance. For instance, the use of a constant convective heat transfer coefficient showed negligible impact on the final structural response (Model 1), while the simplified mechanical theory provided conservative results with a 32% difference in calculated time to collapse compared to the geometrically nonlinear model (Models 2a and 2b). The assumption of two three heat zones increased the time to collapse only by 5%, further division to three (Model 3b) and six zones (Model 3c) increased time to collapse to 12% and 14%, respectively. The variability of axial force significantly influenced collapse time, demonstrating the importance of considering variable axial loads (Models 4a and 4b). The use of standard fire curves resulted in a 3% decrease in collapse time, suggesting that standard fire cure is adequate for analysis in the heating regime (Model 5). Key findings for practitioners:

- Constant convective heat transfer coefficient: Using a constant coefficient from EN 1991-1-2:2002 is safe and does not significantly affect the final structural response.
- Simplified mechanical analysis: This simplification is practical and safe, providing conservative results compared to more precise geometrically nonlinear models.
- Single heat zone: Assuming a single heat zone along the column height is conservative. Using three heat zones offers a more balanced approach without overly conservative results.
- Constant axial force: This assumption is unsafe. Variable axial force should be considered, especially in cases with restrained thermal elongation.
- Standard fire curve: Generally acceptable for routine design. Natural fire curves provide more realistic results in cases with high fire load variability.

By understanding the impact of these simplifications, engineers can make informed decisions to balance safety and efficiency, avoiding unnecessary overdesign while maintaining structural integrity during fire events.

## REFERENCES


[1] EN 1992-1-2:2004, Eurocode 2: Design of concrete structures - Part 1-2: General rules - Structural fire design, European Committee for Standardization, 2004.

[2] EN 1991-1-2:2002, Eurocode 1: Actions on structures - Part 1-2: General actions - Actions on structures exposed to fire, European Committee for Standardization, 2002.

[3] Kolšek, J.: Final report on postdoctoral project Fire-safe accommodation of highly combustible materials in steel-framed structures: Development of models and experimental verification (Project No. Z7-7677, Sponsor: Slovenian Research and Innovation Agency), project website: http://arrs-firesim.zag.si/, 2018 (the report is kept in the personal archives of the autor).

[4] Kolšek, J., Rebec, A.: Analysis of the load-bearing structure after the fire of the ASP building in Jesenice, Fire, 23 (2017) 4, pp. 18-22, accesible at: http://arrs-firesim.zag.si/ajax/DownloadHandler.php?file=2057 (August 9, 2024).

[5] Rogulj, M.: Fire analyses of RC columns: effect of different parameters on final calculation of fire resistance, Master's thesis, University of Split, Faculty of civil engineering, architecture and geodesy, 2022.

[6] EN 1990:2002, Eurocode - Basis of structural design, European Committee for Standardization, 2002.

[7] EN 1991-1-1:2002, Eurocode 1: Actions on structures - Part 1-1: General actions - Densities, self-weight, imposed loads for buildings, European Committee for Standardization, 2002.

[8] EN 1363-1:2020, Fire resistance tests - Part 1: General requirements, European Committee for Standardization, 2020.

[9] EN 1365-4:1999, Fire resistance tests for loadbearing elements - Part 4: Columns, European Committee for Standardization, 1999.

[10] FDS, Fire Dynamics Simulator Version 5.5.3: Users' guide, National Institute of Standards and Technology, 2010.

[11] Matala, A.: Estimation of solid phase reaction parameters for fire simulation, Master's thesis, Halsinki University of Technology, Faculty of Information and Natural Sciences, 2008.

[12] Lautenberger, C., Fernandez Pello, C.: Optimization algorithms for material pyrolysis property estimation, Fire Safety Science, pp. 751-764, 2011.

[13] McGrattan, K., Hostikka, S., Floyd, J., McDermott, R., Vanella, M., Mueller, E.: Fire Dynamics Simulator, Technical reference guide, Volume 1: Mathematical model, National Institute of Standards and technology, USA, 2023.

[14] Hurley, M.: SFPE Handbook of Fire Protection Engineering, 5th edition, Springer, 2016.

[15] Češarek, P., Maglica, M., Češarek Kolšek, J.: On reliability and safety of EC2-proposed simplified methods to fire design of RC columns in real building fires, Structural Safety (in preparation to be submitted to the journal), 2024.

[16] Wang, N., Zhang, M., Kang, P., Zhang, J., Fang, Q., Li, W.: Synergistic effect of graphene oxide and mesoporous structure on flame retardancy of nature rubber/IFR composites, Materials, 11 (2018) 6, pp. 1-13.

[17] Rybinski, G.P. Janowska, M. Jozwiak, M.: Thermal stability and flammability of styrene–butadiene rubber (SBR) composite, Journal of Thermal Analysis and Calorimetry, 113 (2013), pp. 43-52.

[18] Simionescu, T.M., Minea, A.A., Balbis dos Reis, P.N.: Fire Properties of Acrylonitrile Butadiene Styrene Enhanced with Organic Montmorillonite and Exolit Fire Retardant, Applied Sciences, 9 (2019), pp. 1-14.

[19] ABAQUS, Version 6.11, Dassault Systems Simulia Corp., 2011.

[20] EN 1992-1-1:2004, Eurocode 2: Design of concrete structures - Part 1-1 : General rules and rules for buildings, European Committee for Standardization, 2004.

[21] Mostafaei, H.: Hybrid fire testing for assessing performance of structures in fire - Application, Fire Safety Journal, 56(2013), pp. 30-38, https://doi.org/10.1016/j.firesaf.2012.12.003.

[22] Tadić, I.: Fire analysis of RC columns: Accounting for realistic (variable) axial load by modelling a larger part of the structural system, Master's thesis, University of Split, Faculty of civil engineering, architecture and geodesy, 2022.